



ISSN: 0067-2904

Green Synthesis of Reduced Graphene Oxide Nanosheets using Iraqi *Rhus coriaria* (L.) Fruits Extract and a Study of Its Anticancer Activity

Amenah Salim Kadhim¹, Zainab Shakir Abdullah Al-Ali^{2*}

¹Department of Chemistry, College of Science, University of Thi-Qar, Thi-Qar, Iraq

²Department of Chemistry, College of Science, University of Basra, Basra, Iraq

Received: 11/6/2023

Accepted: 9/9/2023

Published: 30/11/2024

Abstract

Ethyl acetate was used to extract bioactive compounds from the fruits of the Iraqi sumac plant *Rhus coriaria*. This sumac fruit extract was then utilized as a natural reducing agent to convert graphene oxide into reduced graphene oxide (rGO) nanosheets through a green synthesis method. Gas chromatography-mass spectrometry (GC-MS) analysis of the ethyl acetate sumac fruit extract identified phytochemicals that likely facilitated the biosynthesis of the rGO nanosheets. The biosynthesized EERCF-rGO was characterized by using UV-Vis 234 nm. FTIR spectrum was used to know functional groups of EERCF-rGO, XRD spectra of EERCF-rGO displayed sized at 26.91 nm, Raman spectra of EERCF-rGO showed D peak at (1335 cm^{-1}) and a G peak at (1592 cm^{-1}). The morphology of EERCF-rGO was determined using FESEM, which offers plates shape. Also, the TEM of EERCF-rGO showed a size at 12 nm. The biosynthesized of EERCF-rGO appeared to have anticancer activity in vitro cytotoxicity by MTT assay, IC_{50} is (189.67 $\mu\text{g/mL}$) against human breast cancer (MCF-7) cell line. The use of biological extracts as reducing agents to produce reduced graphene oxide is an inexpensive, nontoxic, and environmentally friendly approach. The reduced graphene oxide biosynthesized using extracts from the fruits of the Iraqi *Rhus coriaria* plant demonstrated anticancer properties. This method of green synthesis and the resulting anticancer biomaterial show potential for further development.

Keywords: *Rhus coriaria* (L.), Reduced graphene oxide (rGO), Anticancer activity, Biosynthesis, Mechanical biosynthesis.

التخليق الاخضر لأوكسيد الكرافين المختزل استخدام الثمار السماق العراقي ودراسة فعاليته مضاد للسرطان

امنه سالم كاظم¹, زينب شاكر عبدالله ال علي^{2*}

¹القسم الكيمياء, الكلية العلوم, الجامعة ذي قار, ذي قار, العراق

²القسم الكيمياء, الكلية العلوم, الجامعة البصرة, البصرة, العراق

الخلاصة

استخدم خلاص الاثيل لاستخلاص المركبات الحيوية الفعالة من ثمار نبات السماق العراقي *Rhus coriaria* (L.). هذا المستخلص من ثمار السماق كان مفيداً كعامل اختزال طبيعي لتحويل اوكسيد الكرافين

* Email: zainab.abdulah@uobasrah.edu.iq

الى الصفائح النانوية من اوكسيد الكرافين المختزل (rGO) خلال طريقة التخليق الاخضر. شخص جهاز كروماتوغرافيا الغاز- طيف الكتلة لمستخلص خلايا الاثيل لثمار السماق المركبات الكيميائية النباتية التي من الممكن تسهل التخليق الاخضر للصفائح النانوية لاوكسيد الكرافين المختزل. شخص المخلوق الحيوي اوكسيد الكرافين المختزل لمستخلص خلايا الاثيل لثمارالسماق (EERCF-rGO) باستخدام جهاز مطيافية الاشعة المرئية و فوق البنفسجية 234 نانومتر. استخدم طيف الاشعة فوق الحمراء لمعرفة المجاميع الوظيفية لاوكسيد الكرافين المختزل لمستخلص خلايا الاثيل لثمار السماق, اظهر طيف الاشعة السينية حجم اوكسيد الكرافين المختزل لمستخلص خلايا الاثيل لثمار السماق 26.91 نانومتر, اظهر طيف رامان لاوكسيد الكرافين المختزل لمستخلص خلايا الاثيل لثمار السماق حزمة دي (1335 سم⁻¹) وحزمة جي (1592 سم⁻¹). حدد شكل اوكسيد الكرافين المختزل لمستخلص خلايا الاثيل لثمار السماق باستخدام المجهر الالكتروني الماسح الذي اظهر شكل صفائح. كذلك, اظهر المجهر الالكتروني النافذ لمستخلص خلايا الاثيل لثمار السماق حجم 12 نانومتر. اظهر المخلوق الحيوي لاوكسيد الكرافين المختزل لمستخلص خلايا الاثيل لثمار السماق له فعالية مضاد السرطان بواسطة تحليل السمية الخلوية حيث يكون نصف التركيز المثبط (189.67 مايكروغرام/مليمترا) ضد خط خلايا سرطان الثدي البشري (MCF-7). استخدام المستخلصات الحيوية كعوامل اختزال لإنتاج اوكسيد الكرافين المختزل طريقة غير مكلفة, غير سامة و صديقة للبيئة. اظهر اوكسيد الكرافين المختزل المخلوق حيوياً باستخدام مستخلصات من ثمار نبات السماق العراقي خصائص مضاد السرطان. تظهر طريقة التخليق الاخضر والمادة الحيوية المضادة للسرطان الناتجة امكانية لمزيد من التطوير.

1. Introduction

Cancer stands as one of the prevailing fatal illnesses, encompassing variants like breast, lung, and prostate cancers [1-3]. Among them, breast cancer ranks as the second leading cause of female mortality [4]. The World Health Organization (WHO) noted that in 2020, approximately 2.3 million women were afflicted with breast cancer, resulting in around 685,000 fatalities, thus posing a significant global health hazard [5]. To counter this, researchers are exploring nanomaterials as potential agents for cancer treatment, aiming to mitigate harm to healthy cells while addressing this pressing worldwide concern [6]. One of the important nanomaterials is graphene, which is a single layer of graphite, and carbon atoms of graphene have sp² hybridisation, rearranged in a honeycomb lattice [7]. Graphene has good physicochemical features such as large surface area, electrical, chemical, and mechanical properties, and its geometry is two-dimensional and displays an elastic platform for the carrier of different materials, including biomolecules and drugs [8, 9]. Many studies used graphene-based nanomaterial for bio applications as cancer therapy focused on the target cells and minimising side effects [10]. In the realm of cancer treatment, graphene oxide (GO) holds significant promise as a derivative of graphene, a prominent carbon material. This is attributed to its adaptable surface chemistry, enabling easy functionalization, and its exceptional water dispersion capabilities [11]. GO has oxygen functional groups such as epoxide, carboxylic and hydroxyl, making it a special material in biological applications [12]. Another graphene derivative is reduced graphene oxide (rGO), which has the same structure as graphene with little oxygen functional groups on the surface compared with GO [13]. rGO is prepared by many methods, such as chemical reduction, thermal reduction and biological reduction (green synthesis). The chemical reduction approach uses toxic reducing agents such as NaBH₄ and hydroquinone, whereas the thermal reduction approach is not favored because it occurs at room temperature [14]. Biological reduction is the best method compared with other methods because this method is inexpensive, safe, not complex, uses a natural reducing agent and is eco-friendly [15].

For this reason, the green approach has attracted the interest of researchers in rGO preparation, which is used in biomedical applications as antibacterial activity [16] and

anticancer activity [17]. In this study, Iraqi *Rhus coriaria* (L.) fruit extract was used as bio reducing agent to synthesis reduced graphene oxide (rGO). In an effort to unravel the proposed bioreduction mechanism of reduced graphene oxide (rGO), this stage involves identifying phytochemical structures using GC/MS spectra. In addition, it investigates *Rhus coriaria*-rGO the medical abilities, as anticancer activity against breast cancer (MCF-7) cell lines.

2. Materials and Methods

2.1. Synthesis of graphene oxide (GO)

The enhanced Hummer technique [18]. is employed to synthesize graphene oxide. In this method, a mixture containing 360 mL of concentrated sulfuric acid (H_2SO_4) with a molarity of 18.41 M and 40 mL of concentrated orthophosphoric acid (H_3PO_4) with a molarity of 15.18 M is prepared in a 9:1 ratio. This mixture is then stirred. Following this, 3 g of graphite powder is introduced into the mixture, and subsequently, a slow addition of 18 g of potassium permanganate ($KMnO_4$) is initiated while maintaining continuous stirring. This process results in the solution turning into a deep green hue. The reaction mixture was placed in an ice bath with salt and monitored using a thermometer to maintain a temperature of $50^\circ C$ with stirred for 12 h. The reaction was cooled to room temperature and poured on 400 mL of ice with 3 mL of (30% H_2O_2). The formed solution was yellow. It was then sifted through a sieve and filtered through polyester fabric. A sieve is placed on top of a polyester cloth; the mixture is poured into the sieve; the mixture is filtered through the sieve; then the polyester cloth is used to form a soft and easy fabric known as (Mellmal). After that, the filtrate was centrifuged (4000 rpm for 4 h) while the supernatant decanted away, the precipitating material washed in 200 mL of water, 200 mL of 30% hydrochloric acid (HCl) and 200 mL of ethanol (two times the process was repeated). The product was collected, coagulated with 200 mL of ether, and filtered through filter paper (Whatman no1). The product obtained on the filter was vacuum-dried overnight at room temperature.

2.2. Plant material and extract preparation

In August 2021, fruits of *Rhus coriaria* (L.) were gathered within Chamchamal City, located in Sulaymaniyah, Iraq. Subsequently, the collected fruits underwent a thorough washing process, involving rinsing with water and deionized water (D.I.), with this step being repeated twice. After washing, the fruits were subjected to a drying period of three days at room temperature, away from direct light. Following this, the dried fruits were processed into a powdered form using a blender. The resulting powder was then stored at a temperature of $4^\circ C$ until it was ready for utilization.

2.3. Preparation of ethyl acetate extract of *Rhus coriaria* (L.) fruit (EERCF)

Ethyl acetate extract of *Rhus coriaria* (L.) fruits (EERCF) was prepared following a modified procedure [19]. Fruits powder of (10 g) was mixed with 100 mL of (70% ethyl acetate) and stirred at $40^\circ C$ for 30 min; cooled and filtered the solution using a Büchner funnel that separated the extract from the solid material. The filter was combined and used a rotary evaporator at $40^\circ C$ until dryness. The dry powder (solid residue) is stored in use.

2.4. Green synthesis of reduced graphene oxide (EERCF-rGO)

For the biosynthesis of reduced graphene oxide nanosheets (EERCF-rGO), begin by dissolving 0.04 g of graphene oxide (GO) in 100 mL of distilled water. Next, introduce 0.01 g of dried ethyl acetate extract from Iraqi *Rhus coriaria* (L.) fruit into the solution. Subsequently, subject the mixture to sonication for a duration of 40 minutes [20]. The yellowish-brown GO solution was refluxed at $95^\circ C$ in a water bath for 12 h. After that, GO's yellowish-brown colour converted to black, evidence of success in removing oxygen groups

of GO. According to the change of energy levels which attributed to the change of material color. Before the reduction, the GO included the oxygen groups on graphene sheets (free electrons and π electrons) after reduction the oxygen groups is removed by bioreduction which increased π electrons concentration and rearrangement of sp^2 carbon network [21]. The black colour mixture was centrifuged at 10000 rpm for 10 min. The remaining material was washed with deionized water (D.I.) and dried. The black powder of EERCF-rGO was stored in the vial for furthermore studies.

2.5. Characterization Techniques

The samples of GO and biosynthesized EERCF-rGO were characterized through the following instruments by UV-Visible spectroscopy (UV-1900, Shimadzu, Japan), Fourier-transform infrared spectroscopy (FTIR) determined the wavenumber range of (4000-400 cm^{-1}) (IRAffinity-1800, Shimadzu, Japan), X-ray diffraction by (PW173, PHILIPS, Holanda). Raman spectroscopy (TahranN1-541, TESCAN, Iran). Field emission scanning electronic microscopic (FESEM) images were obtained by using (MIRA III, TESCAN, Czech), Transmission electron microscopy (TEM) (Libra 120, CarZeiss, Germany), GC-MS analysis (Agilent 7820A, USA).

2.6. Cytotoxicity MTT assay of EERCF-rGO

With some modifications, the EERCF-rGO cytotoxicity was determined during the MTT assay [22]. The cell line (MCF-7) was cultured at a 96-well plate at a 1×10^5 cell/well for 24 hours at optimal conditions (37°C, 5% CO_2 in humidified incubator). Next, the growth media (10% FBS) was removed, and the cells were washed two times with phosphate buffer saline (PBS). New maintenance RPMI medium (10% FBS) containing (12.5, 25, 50, 100 and 200 $\mu g/mL$) of EERCF-rGO was added, and the cells were incubated for 72 h. Triple wells were analysed for each concentration, and column elution buffer was used as the control. A 10 μL solution of freshly prepared 5 mg/mL MTT in PBS was added to each well and incubated for 4 h. The media was removed, and DMSO was added at 100 $\mu L/well$. Plates were shaken gently to facilitate formazan crystal solubilisation (Formazan dyes are purple-colored crystals insoluble that are obtained by reducing tetrazolium salts by mitochondrial enzymes in living cells). The absorbance was measured at 545 nm using a microplate reader. The control group's mean optical absorbance was set to 100%, and the optical absorbance of the other examinational groups was calculated as a percentage of the control group's value. The percentage of cell toxicity and half-maximal inhibitory concentration (IC_{50}) were calculated.

3. Results and Discussion

3.1. UV-Vis spectroscopy

In the UV-Vis spectra of EERCF-rGO, a distinctive peak was observed at 234 nm, signifying a redshift from the absorbance peak seen at 226 nm in the GO spectra. Conversely, the GO spectra exhibited a peak at 226 nm along with a secondary peak at 296 nm. These peaks were indicative of the $\pi-\pi^*$ electronic transition occurring within the aromatic C=C bonds and were attributed to the $n-\pi^*$ transition of the aromatic C=O bonds within the carbonyl group, respectively. This observation aligns with prior research findings, further validated by a comparative analysis with existing studies [23, 24]. Also, graphite spectra showed a weak peak at 282 nm, which indicated the $\pi-\pi^*$ electronic transition of the C=C bonds at this peak [25], (see Figure 1).

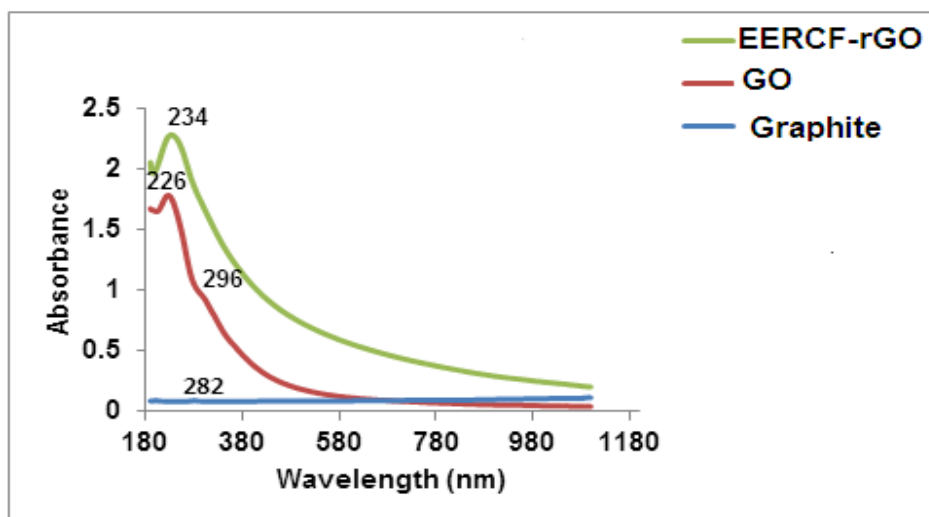


Figure 1: UV-Vis spectroscopy of graphite, GO, EERCF-rGO.

3.2. FTIR spectra

The FTIR spectrum of graphite, GO, EERCF-rGO appeared a very low-intensity band at 1639 cm^{-1} , which indicated the stretching vibration of the C=C bond and formed the carbon structure of graphite [26]. Where the FTIR spectra of GO observed a wide peak centred at 3360 cm^{-1} and another peak at 1454 cm^{-1} , these peaks were due to the stretching vibration and bending vibration of the hydroxyl groups (OH), respectively, which attributed to the water molecules adsorbed on the surface of GO, this confirms the hydrophilic natural of GO [27]. Moreover, the spectrum showed bonds at 2920 cm^{-1} and 2850 cm^{-1} , 1739 cm^{-1} , 1620 cm^{-1} , 1222 cm^{-1} and 1053 cm^{-1} , which are attributed to the stretching vibration of aliphatic (C-H), carbonyl groups (C=O) stretching of carboxyl (COOH), (C=C) stretching [28, 29]. Finally (C-O) stretching of alkoxy and epoxy, respectively [30]. After the reduction process by ethyl acetate extract Iraqi *Rhus coriaria* (L.) fruits. The FTIR spectra of EERCF-rGO showed peaks at 3298 cm^{-1} and 1396 cm^{-1} , which represented the stretching vibration and binding vibration of hydroxyl groups (O-H) [31]; these peaks were lower intensity than the peaks of hydroxyl groups in GO spectra. The peak at 1631 cm^{-1} was attributed to the stretching vibration C=C band, which is shifted to a high wavenumber compared with the band C=C wavenumber of GO spectra [32]. Also, the peak at 1099 cm^{-1} indicates the stretching vibration of the alkoxy group that decreased in wavenumbers compared with GO spectra [33]. The peak at 1739 cm^{-1} in GO spectra disappeared in rGO spectrum; this confirmed the successful reduction of GO by the ethyl acetate extract *Rhus coriaria* (L.) fruits [34], as shown in Figure 2.

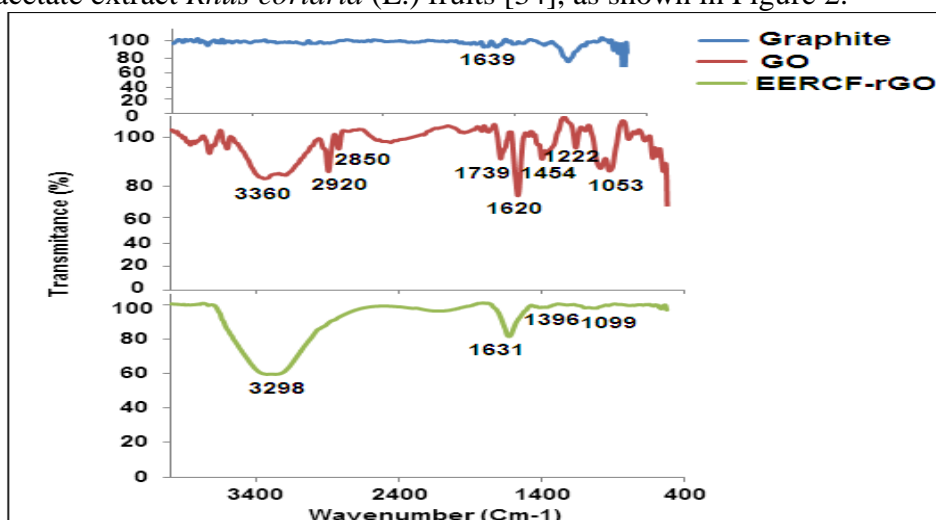


Figure 2: FTIR spectra of graphite, GO, EERCF-rGO.

3.3. X-ray diffraction analysis (XRD)

Figure 3 displays the XRD patterns for graphite, GO, and EERCF-rGO. In the XRD pattern of graphite, the notable high-intensity and well-defined peak at $2\theta = 26.68^\circ$ corresponds to an interlayer spacing of 0.334 nm. This specific spacing is attributed to the organized layer structure of graphite [35]. Also, XRD of GO explained peak at $2\theta = 11.42^\circ$ with a layer spacing between two patterns due to the entrance of water molecules between the graphite layers and the formation of oxygenated functional groups [36]. The XRD of EERCF-rGO appears in the many peaks at 22.9° , 29.83° , 40.79° and 43.46° respectively. The peak centred at 22.9° with a d-spacing of 0.388 nm, and the size was 26.91 nm; this peak indicates to the reduction of GO which almost the same as the following reference [37]. The decreasing d-spacing value of rGO affirmed the loss of oxygen groups [38]. The size of samples was calculated through Scherrer's equation as shown in (1)

$$D = \frac{K \lambda}{\beta \cos \theta} \quad (1)$$

Where D= Crystal size, nm; K= Constant equal, 0.9; λ = wavelength , 0.154 nm; β = FWHM (Full width at half maximum intensity), radians; θ = Bragg angle

The size of samples was calculated by Scherrer's equation and as shown in Table 1.

Table 1: XRD data of graphite, GO and EERCF-rGO

Samples	2θ	FWHM	d-spacing (nm)	Crystal size (nm)
Graphite	26.68	0.2952	0.334	28.90
GO	11.42	0.8004	0.789	10.42
EERCF-rGO	22.9	0.2952	0.388	26.91

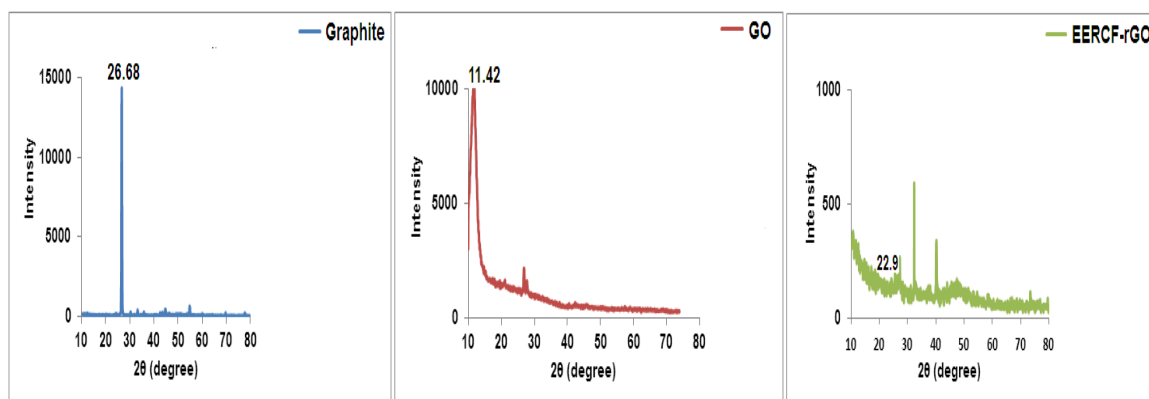


Figure 3: XRD patterns of graphite, GO and EERCF-rGO.

3.4. Raman spectroscopy

The Raman spectra of graphite, graphene oxide (GO) and ethyl acetate extract *Rhus coriaria* (L.) fruits (EERCF-rGO) explain in Figure 4. The Raman spectrum of graphite appears in the G, D and 2D bands 1576 cm^{-1} , 1330 cm^{-1} and 2688 cm^{-1} , respectively [39]. The Raman spectra for GO the G band is broadened and shifted to 1597 cm^{-1} because of the isolation of the double bonds that have higher frequencies than the G bands of graphite [40]. The D band at 1353 cm^{-1} is increased which is indicated by the decrease of the in-plane sp^2 domain size corresponding to the oxidation and ultrasonic exfoliation. Further, the Raman spectra after the GO reduction using the *Rhus coriaria* (L.) fruits extract explained the G band at 1592 cm^{-1} and the D band at 1335 cm^{-1} , respectively [41]. The intensity value ratio (I_D/I_G) measures the sp^2 domain size in the carbon structure, including sp^3 and sp^2 bonds [42]. This ratio (I_D/I_G) was determined in graphene oxide (0.84) to (1.04) in the green synthesized EERCF-rGO, which indicates the recovery of the structure of graphite in the graphene oxide sheets by the reduction.

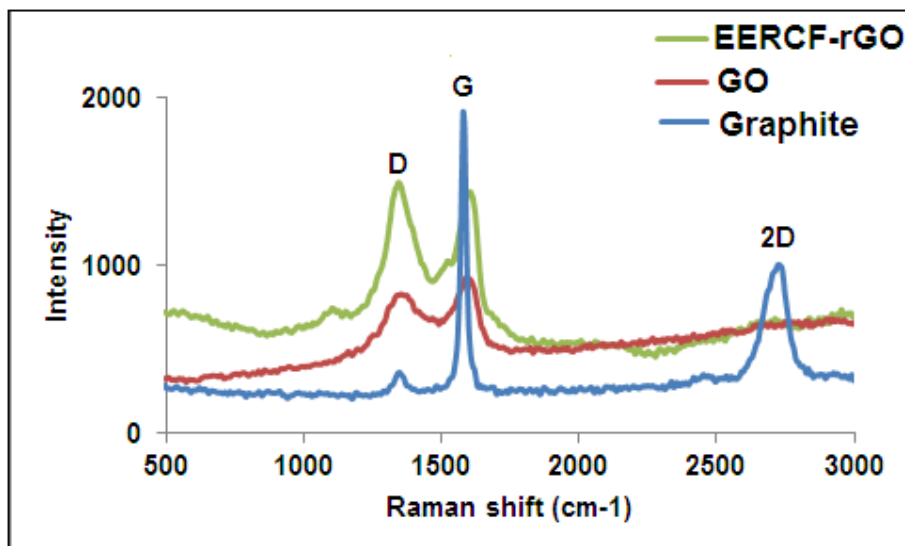


Figure 4: Raman spectra of graphite, GO and EERCF-rGO.

3.5. Field emission scanning electron microscope (FESEM)

When examining the morphology of GO and EERCF-rGO through FESEM analysis, the surface of GO exhibits a folded sheet structure with a textured, wrinkled appearance, resembling the pattern of a wavy carpet. When the measurement zoomed to a small nanoscale that showed the thickness at the range of (14.11 nm- 30.59 nm), the sheets became freer to move due to the intercalation of the oxygen functional groups (epoxy, carboxylic and hydroxyl) on the surface GO through the oxidation process [43, 44]. Whereas the surface of EERCF-rGO explained plates with edges length ranging between (34.1 nm – 66.9 nm), as shown in Figure 5.

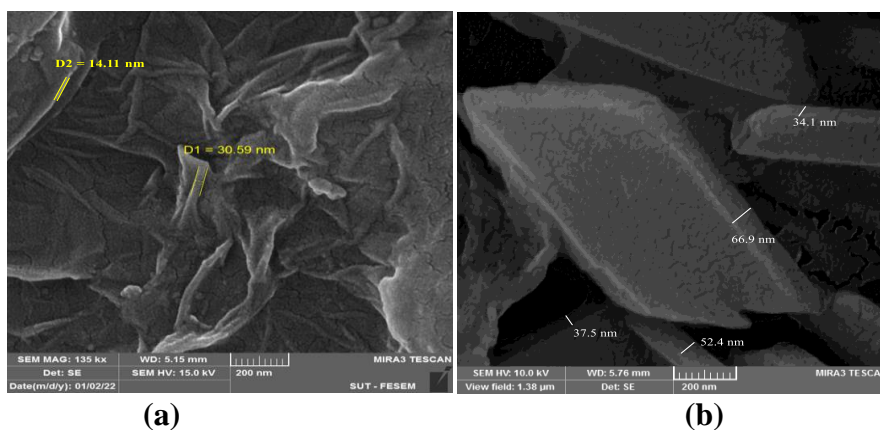


Figure 5: FESEM images of (a) GO and (b) EERCF-rGO.

3.6. Transmission electron microscopy (TEM)

The TEM images of the synthesized graphene oxide (GO) distinctly reveal sheet-like structures upon closer examination, elucidating both the presence of a wrinkled surface and a size measuring 15.54 nm. In contrast, the TEM image of EERCF-rGO illustrates a superimposed plate-like arrangement characterized by graphene layers, exhibiting a transparent yet intricately wrinkled appearance with multiple edges. The maximum thickness observed is 12 nm, as depicted in Figure 6.

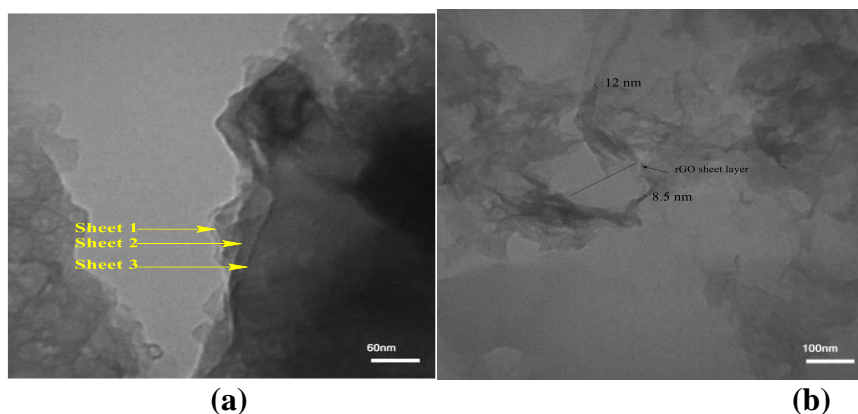


Figure 6: TEM images of (a) GO and (b) EERCF-rGO.

3.7. GC/MS analysis of ethyl acetate extract Iraqi *Rhus coriaria* (L.) fruits

The resulting extract was undergone to GC/MS analysis. The ethyl acetate extract from Iraqi *Rhus coriaria* (L.) fruits of GC/MS spectra revealed 25 compounds. This extract consisted the different classifications of compounds such as, essential oils (50.65%) followed by essential oils esters (32.91%), Polyphenols (1.13%), Ketones (9.69%), Aldehydes (2.1%), Alcohols (1.21%), Ethers (1.18%) and Cyclic amide (1.41%), as shown in Figure 7. Fatty acids: the major component of this class was Oleic acid (36.10%); n-Hexadecanoic acid (6.71%); Octadecanoic acid (4.20%); 9, 12-Octadecadienoic acid (Z, Z) (2.45%); 2-Tridecenoic acid, (E) (0.66%); Cis-vaccenic acid (0.53%). Essential oils esters: which presented the high percentage after the essential oils: 9-Octadecenoic acid, methyl ester,(E) (11.14%); 9,12-Octadecadienoic acid, methyl ester (5.46%); 11-Octadecenoic acid, methyl ester (5.16%); Hexadecanoic acid, methyl ester (5.14%); 9,12-Octadecadienoic acid (Z, Z), methyl ester (3.89%); 3-Trifluoroacetoxypentadecane (0.84%); Acetic acid, hydroxyl, ethyl ester (0.72%) and 4-Trifluoroacetoxytridecane (0.56%). The three class was Polyphenols: which include large groups of compounds such as phenolic acid, flavonoid etc. Gallic acid (0.51%) and Myricetin (0.62%). The fourth class of compounds in EERCF was Ketones: Octahydropyrano[3,2-b]pyridine-6-one (9.13%); 2,4,6-Cycloheptatrien-1-one,3,5-bis-trimethylsilyl (0.56%). The fifth class of compounds in EERCF was Aldehydes: Cyclobarbitol (0.98%); 2,4-Decadienal (0.57%), Cis-11-hexadecenal (0.55%). The sixth class of compounds in EERCF was Ethers: Benzene alcohol, and benzyl dimethylsilyl ether (1.18%). The seventh class of compounds in EERCF was Alcohol: Stigmasterol (0.7%) and 2-Methyl-Z,Z-3,13-octadecadienol (0.51%). Finally, the eighth class was Cyclic amides: Caprolactam (1.14%), as shown in Table 2.

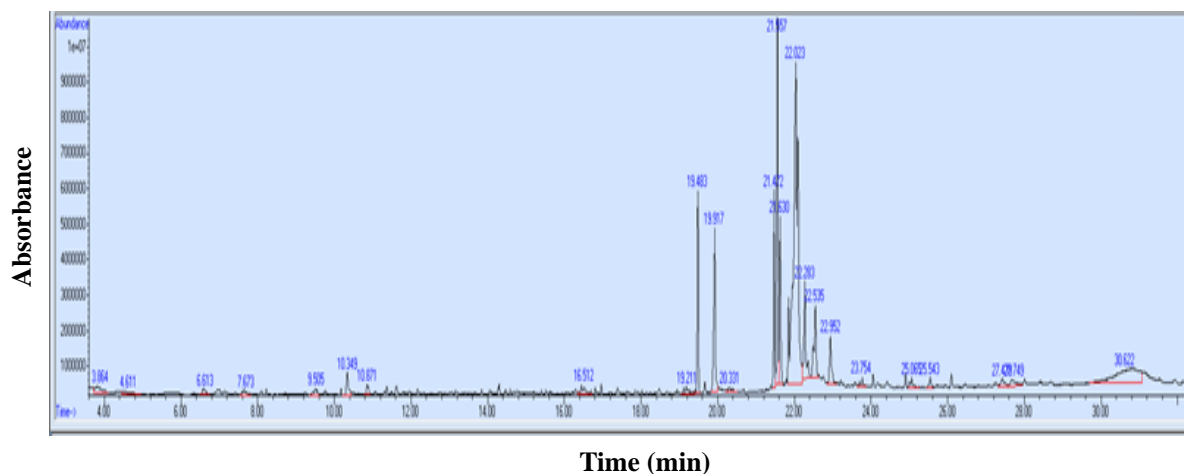
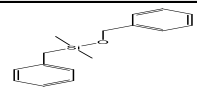
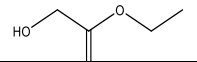
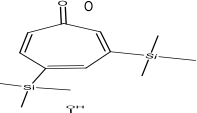
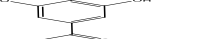

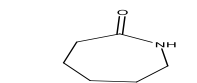
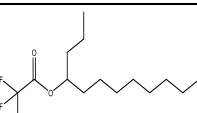
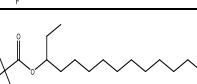
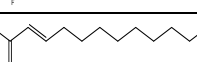
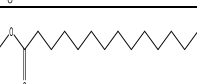
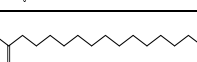
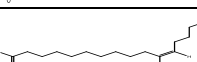
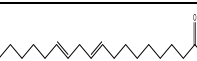


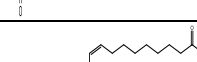
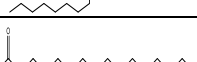

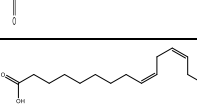
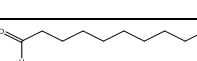
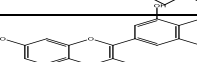
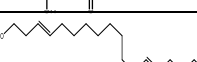

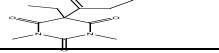
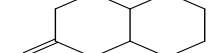


Figure 7: GC/MS chromatogram of an ethyl acetate extract of *Rhus coriaria* (L.) fruits.

Table 2: GC/MS screening of the phytochemicals present in ethyl acetate extract Iraqi *Rhus coriaria* (L.) fruits.

NO	Retention time (min)	Area of peak (%)	Compound identified	Molecular formula	M.W. (g/mol)	Structure
1	3.684	1.18	Benzyl alcohol, benzyl dimethyl silyl ether	C ₁₆ H ₂₀ OSi	256.41	
2	4.611	0.72	Acetic acid, hydroxy, ethyl ester	C ₄ H ₈ O ₃	104.10	
3	6.13	0.56	2,4,6-Cycloheptatrien-1-one,3,5-bis-trimethylsilyl	C ₁₃ H ₂₂ OSi ₂	250.48	
4	7.673	0.51	Gallic acid	C ₇ H ₆ O ₅	170.12	
5	9.505	0.57	2,4-Decadienal	C ₁₀ H ₁₆ O	152.23	
6	10.349	1.14	Caprolactam	C ₆ H ₁₁ NO	113.16	
7	10.871	0.56	4-Trifluoroacetoxytridecane	C ₁₅ H ₂₇ F ₃ O	296.37	
8	16.512	0.84	3-Trifluoroacetoxydecane	C ₁₇ H ₃₁ F ₃ O ₂	324.42	
9	19.211	0.66	2-Tridecenoic acid, (E)	C ₁₃ H ₂₄ O ₂	212.33	
10	19.483	5.14	Hexadecanoic acid, methyl ester	C ₁₇ H ₃₄ O ₂	270.45	
11	19.917	6.71	n- Hexadecanoic acid	C ₁₆ H ₃₂ O ₂	256.42	
12	20.331	0.53	Cis- Vaccenic acid	C ₁₈ H ₃₄ O ₂	282.5	
13	21.462	5.46	9,12-Octadecadienoic acid, methyl ester	C ₁₉ H ₃₄ O ₂	294.47	
14	21.557	11.14	9-Octadecenoic acid, methyl ester, (E)	C ₁₉ H ₃₆ O ₂	296.48	
15	21.630	5.16	11-Octadecenoic acid, methyl ester	C ₁₉ H ₃₆ O ₂	296.48	
16	22.023	36.10	Oleic acid	C ₁₈ H ₃₄ O ₂	282.46	
17	22.283	4.20	Octadecanoic acid	C ₁₈ H ₃₆ O ₂	284.47	
18	22.535	3.89	9,12-Octadecadienoic acid-(Z,Z)-methyl ester	C ₁₉ H ₃₄ O ₂	294.47	
19	22.952	2.45	9,12-Octadecadienoic acid (Z,Z)	C ₁₈ H ₃₂ O ₂	280.45	
20	23.754	0.55	Cis-11-hexadecenal	C ₁₆ H ₃₀ O	238.41	
21	25.065	0.62	Myricetin	C ₁₅ H ₁₀ O ₈	318.23	
22	25.546	0.51	2-methyl-Z,Z-3,13-Octadecadienol	C ₁₉ H ₃₆ O	280.5	

23	27.441	0.70	Stigmasterol	C ₂₉ H ₄₈ O	412.7	
24	27.749	0.98	Cyclobarbitol	C ₁₂ H ₁₆ N ₂ O	236.27	
25	30.622	9.13	Octahydropyrano[3,2-b]pyridine-6-one	C ₁₈ H ₁₃ NO ₂	155.19	

Recent studies showed essential oils are considered interesting biosources in the medical field and play an important role in reducing and capping agents for biosynthesized silver and gold nanoparticles [45, 46]. According to the scientific literature [47], the suggested mechanism pathway for essential oils extracted from *Rhus coriaria* (L.) fruits can be seen in Figure 8. *Rhus coriaria* (L.) extract and specifically Iraqi *Rhus coriaria* (L.) fruits extract have not been used as reducing agents for the reduction of GO, There are essential oils in Iraqi *Rhus coriaria* (L.) fruits, of which oleic acid has the highest percentage (36%). All of these essential oils contain a carboxylic functional group in their structure, which is represented by the shape. The surface of graphene oxide (GO) contains a variety of oxygen groups, including epoxides, carboxylic and hydroxyls. Protonation activates the carbonyl of the carboxylic group of essential oils in the first step. A hydroxyl group (OH) of essential oils attacked the epoxy group on GO, causing the epoxy ring to open and form a hydroxyl group (oxygen of the epoxy group takes hydrogen of the hydroxyl group from essential oils). The water molecule is removed after the hydroxyl group on the GO surface takes hydrogen from hydroxyl group (⁺OH) of essential oils, creating a new ring. Afterwards, the bonds are cleaved to create reduced graphene oxide (rGO). In the condensation reaction, the hydroxyl group of essential oils attacked the carboxylic group of GO, which formed a new bond and released water. The bonds replaced the places by resonance, and the bonds were cleaved to result in rGO. As the hydroxyl group of essential oils attacked the hydroxyl group of GO, the water molecule was lost, the bonds were rearrangement to form a new ring. As a result of the new bond cleavages, rGO is produced.

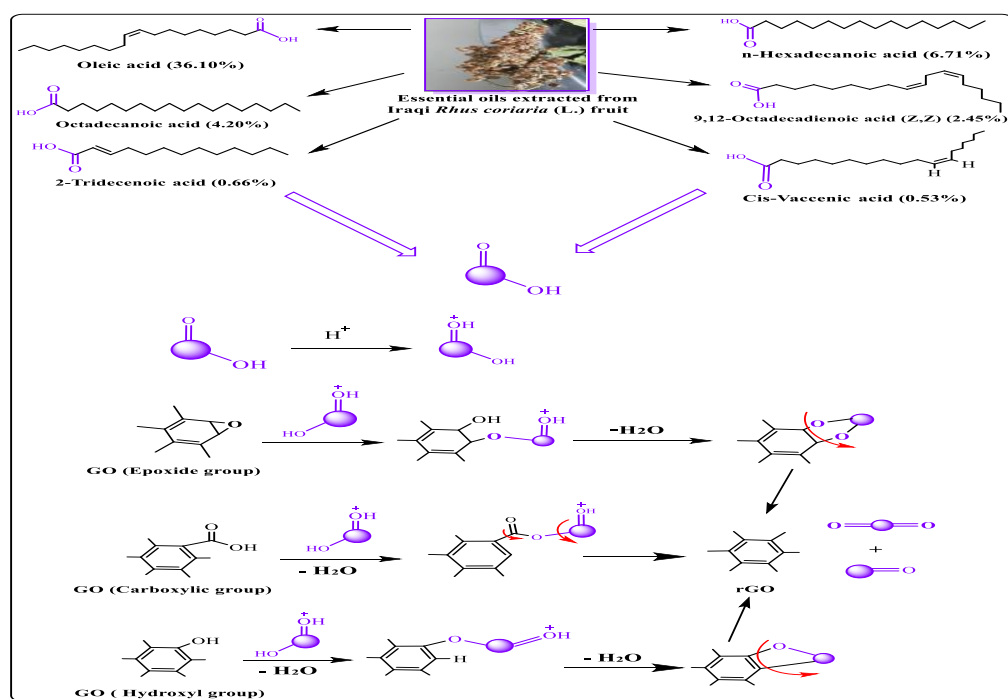


Figure 8: The suggested mechanism for the green synthesis of rGO using the essential oils from ethyl acetate extract of Iraqi *Rhus coriaria* (L.) fruits.

3.8. MTT assay

The anticancer potential of reduced graphene oxide biosynthesized with *Rhus coriaria* fruit extract (EERCF-rGO) was evaluated against MCF-7 breast cancer cell lines. Treatment with increasing concentrations of EERCF-rGO from 12.5 to 200 $\mu\text{g/mL}$ led to a concentration-dependent decrease in MCF-7 viability from 90.25% to 51.88%, respectively. This demonstrates a clear concentration-dependent anticancer effect of EERCF-rGO against the breast cancer cells. The green synthesis of graphene oxide using natural plant extracts like *R. coriaria* provides a sustainable approach for producing anticancer biomaterials (see Figure 9). The IC_{50} of ethyl acetate extract *Rhus coriaria* (L.) fruit-rGO (EERCF-rGO) was determined at 189.67 $\mu\text{g/mL}$. The graphene-based material as rGO binds to the cell membrane, can generate reactive oxygen species (ROS) in the cell [48]. Overall, the cell balance desaturation, the ROS cumulated in the cell that causes DNA damage and mitochondrial dysfunction [49]. Cytotoxicity of graphene nanomaterials depends on their size, functional group density, and cell type. Graphene nanomaterials cytotoxicity is affected by their functional group density. Reduced graphene oxide (EERCF-rGO) is one of these graphene nanomaterials, so its cytotoxicity is dependent upon these factors. EERCF-rGO sheets were functionalized by phytochemicals of *Rhus coriaria* (L.) fruits extract (essential oils and polyphenols), decreasing cell viability and increasing the inhabitation rate [50].

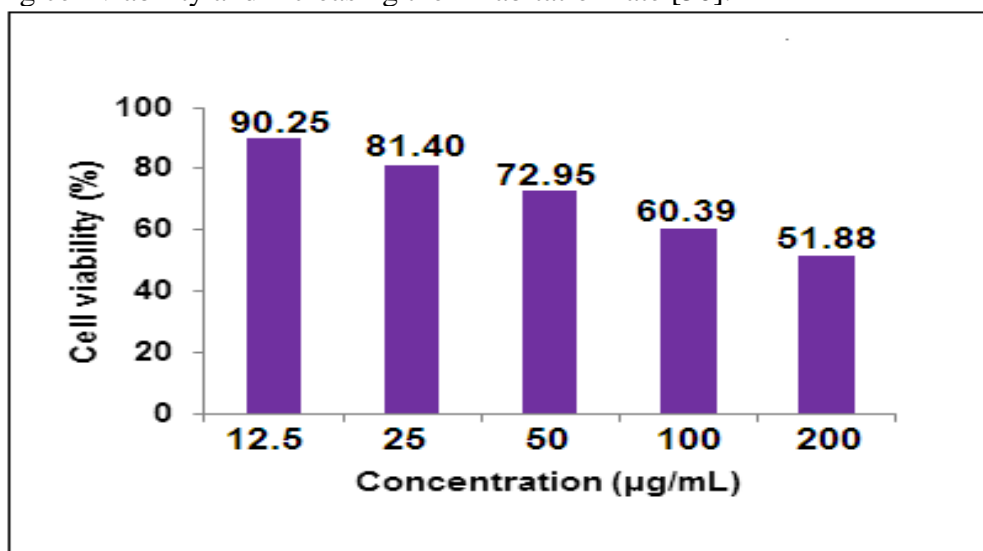


Figure 9: The cell viability of MCF-7 cells after treatment with EERCF-rGO.

Conclusion

An Iraqi *Rhus coriaria* (L.) fruits extract was successfully used in the biosynthesis of reduced graphene oxide (rGO) from graphene oxide (GO), marking the first use of *Rhus coriaria* (L.) fruits extract for reduced graphene oxide (rGO) biosynthesis. Essential oils were used to synthesize rGO, which is regarded as a good source for green synthesis. Imaging techniques like field emission scanning electron microscopy (FESEM) and transmission electron microscopy (TEM) revealed that the EERCF-rGO material consisted of layered nanosheets. X-ray diffraction (XRD) analysis determined the crystalline size of EERCF-rGO to be 26.91 nm, while TEM imaging showed the nanosheet thickness to be around 12 nm. Additionally, Raman spectroscopy confirmed the successful formation of EERCF-rGO nanosheets. With breast cancer posing a major global health burden, green-synthesized nanomaterials like EERCF-rGO may offer alternative treatment options to conventional therapies. The anticancer activity demonstrated against MCF-7 breast cancer cell lines highlights the potential of plant-derived graphene oxide nanosheets as safer, sustainable therapeutics. Based on the MTT assay, the biosynthesized EERCF-rGO inhibited the growth of the human breast cancer cell lines (MCF-7).

Conflicts of Interest

The authors declare that they have no conflicts of interest.

Acknowledgements

The authors thank the Ciате biologist of Mustansiriyah University, Qabas Nather, who has helped and provided the plant (*Rhus coriaria* (L.)) fruits for this study.

References

- [1] W. Choi and E. S. Lee, "Therapeutic targeting of DNA damage response in cancer", *International Journal of Molecular Sciences*, vol. 23, no. 1701, pp. 1-28, 2022.
- [2] S. H. Hassanpour, and M. Dehghani, "Review of cancer from perspective of molecular", *Journal of cancer research and practice*, vol. 4, no. 4, pp. 127-129, 2017.
- [3] S. Rajeshkumar, "Anticancer activity of eco-friendly gold nanoparticles against lung and liver cancer cells", *Journal of Genetic Engineering and Biotechnology*, vol. 14, no. 119729, pp. 195-202, 2016.
- [4] H. Nagai, and Y. H. Kim, "Cancer prevention from the perspective of global cancer burden patterns", *Journal of Thoracic Disease*, vol. 9, no. 3, pp. 448-451, 2017.
- [5] M. Arnold, E. Morgan, H. Rumgay, A. Mafra, D. Singh, M. Laversanne, J. Vignat, J. R. Gralow, F. Cardoso, and S. Siesling, "Current and future burden of breast cancer: Global statistics for 2020 and 2040", *The Breast*, vol. 66, no. 8, pp. 15-23, 2022.
- [6] U. Munawer, V. R. Raghavendra, S. Ningargju, K. L. Krishna, A. R. Ghosh, G. Melappa, and A. Pugazhenhi, "Biofabrication of gold nanoparticles mediated by the endophytic cladosporium species: photodegradation, in vitro anticancer activity and in vitro antitumor studies", *International Journal of Pharmaceutics*, vol. 588, no.119729, pp. 1-12, 2020.
- [7] M. H. Al-Abboodi, F. N. Ajeel, and A. M. Khudhari, "Influence of oxygen impurities on the electronic properties of graphene nanoflakes", *Physica E: Low-Dimensional Systems and Nanostructures*, vol. 88, no. 6, pp. 1-5, 2017.
- [8] T. A. Salaheldin, S. A. Loutfy, M. A. Ramadan, T. Youssef, and S. A. Mousa, "IR-enhanced photothermal therapeutic effect of graphene magnetite nanocomposite on human liver cancer HepG2 cell model", *International Journal of Nanomedicine*, vol. 14, pp. 4397-4412, 2019.
- [9] H. Al-Sagur, E. Kaya, M. Durmuş, T. Basova, and A. Hassan, "Amperometric glucose biosensing performance of a novel graphene nanoplatelets-iron phthalocyanine incorporated conducting hydrogel", *Biosensors and Bioelectronics*, vol. 139, no. 111323, pp. 1-7, 2019.
- [10] H. -Y. Fan, X. -H. Yu, K. Wang, Y. J. Yin, Y. -J. Tang, Y. -I. Tang, and X. -H. Liang, "Graphene quantum dots (GQDs)-based nanomaterials for improving photodynamic therapy in cancer treatment", *Eurpoen Journal of Medicinal Chemistry*, vol. 182, no. 111620, pp.1-11, 2019.
- [11] D. P. Singh, C. E. Herrera, B. Singh, S. Singh, R. K. Singh and R. Kumar, "Graphene oxide: An efficient material and recent approach for biotechnological and biomedical applications", *Materials Science and Engineering: C*, vol. 86, no. 1, pp. 137-197, 2018.
- [12] G. Cui, J. Wu, J. Lin, W. Liu, P. Chen, M. Yu, D. Zhou, and G. Yao, "Graphene-based nanomaterials for breast cancer treatment: promising therapeutic strategies", *Journal of Nanobiotechnology*, vol. 19, no. 1, pp. 1-3, 2021.
- [13] D. F. Báez, H. Pardo, I. Laborda, J. F. Marco, C. Yáñez, and S. Bollo, "Reduced graphene oxides: influence of the reduction method on the electrocatalytic effect towards nucleic acid oxidation", *Nanomaterials*, vol. 7, no. 168, pp. 1-15, 2017.
- [14] R. K. Singh, R. Kumar, and D. P. Singh, "Graphene oxide: strategies for synthesis, reduction and frontier applications", *Rsc Advances*, vol. 6, no.69, pp.64993-65011, 2016.
- [15] M. J. -Y. Tai, W. W. Liu, C. S. Khe, N. Hidayah, Y. -P. Teoh, C. Voon, H. C. Lee, and P. Adelyn, "Green synthesis of reduced graphene oxide using green tea extract", *AIP Conference Proceedings*, vol. 2045, no. 1, pp. 020032, 2018.

- [16] M. N. Rani, S. Ananda, and D. Rangappa, "Preparation of reduced graphene oxide and its antibacterial properties". *Materials Today: Proceedings*, vol. 4, no. 11, pp. 12300-12305, 2017.
- [17] X. Zhu, X. Xu, F. Liu, J. Jin, L. Liu, Y. Zhi, Z. -W. Chen, Z. -S. Zhou, and J. Yu, "Green synthesis of graphene nanosheets and their in vitro cytotoxicity against human prostate cancer (DU 145) cell lines". *Nanomaterials and Nanotechnology*, vol. 7, no. 1847980417702794, pp. 1-7, 2017.
- [18] D. C. Marcano, D. V. Kosynkin, J. M. Berlin, A. Sinitskii, Z. Sun, A. Slesarev, L. B. Alemany, W. Lu, and J. M. Tour, "Improved synthesis of graphene oxide". *ACS Nano*, vol. 4, no. 8, pp. 4806-4814, 2010.
- [19] T. Mazaheri, M. Hesarinejad, S. Razavi, R. Mohammadian, and S. Poorkian, "Comparing physicochemical properties and antioxidant potential of sumac from Iran and Turkey". *MOJ Food Process Technol*, vol. 5, no. 2, pp. 288-294, 2017.
- [20] N. Thiagarajulu, S. Arumugam, A. L. Narayanan, T. Mathivanan, and R. R. Renuka, "Green synthesis of reduced graphene nanosheets using leaf extract of *tridax procumbens* and its potential in vitro biological activities". *Biointerface Research in Applied Chemistry*, vol. 11, no. 3, pp. 9975-9984, 2020.
- [21] S. Thakur, and N. Karak, "Green reduction of graphene oxide by aqueous phytoextracts". *Carbon*, vol. 50, no. 14, pp. 5331-5339, 2012.
- [22] P. Punniyakotti, R. Aruliah, and S. Angaiah, "Facile synthesis of reduced graphene oxide using *Acalypha indica* and *Raphanus sativus* extracts and their in vitro cytotoxicity activity against human breast (MCF-7) and lung (A549) cancer cell lines". *3 Biotech*, vol. 11, no. 157, pp. 1-11, 2021.
- [23] S. Ahmad, A. Ahmad, S. Khan, S. Ahmad, I. Khan, S. Zada, and P. Fu, "Algal extracts based biogenic synthesis of reduced graphene oxide (rGO) with enhanced heavy metals adsorption capability". *Journal of Industrial and Engineering Chemistry*, vol. 72, no. 2019, pp. 117-124, 2019.
- [24] A. Barjola, M. A. Tormo-Mas, O. Sahuquillo, P. Bernabé-Quispe, J. M. Pérez, and E. Giménez, "Enhanced antibacterial activity through silver nanoparticles deposited onto carboxylated graphene oxide surface". *Nanomaterials*, vol. 12, no. 1949, pp. 1-22, 2022.
- [25] F. Fauzi, F. Azizi, M. M. Musawwa, and W. S. B. Dwandaru, "Synthesis and characterisations of reduced graphene oxide prepared by microwave irradiation with sonication". *Journal of Physical Science*, vol. 32, no. 2, pp. 1-13, 2021.
- [26] T. Kuila, S. Bose, P. Khanra, A. K. Mishra, N. H. Kim, and J. H. Lee, "A green approach for the reduction of graphene oxide by wild carrot root". *Carbon*, vol. 50, no. 3, pp. 914-921, 2012.
- [27] S. Parrek, D. Jain, R. Shrivastava, S. Dam, S. Hussain and D. Behera, "Tunable degree of oxidation in graphene oxide: cost effective synthesis, characterization and process optimization". *Materials Research Express*, vol. 6, no. 8, pp. 1-15, 2019.
- [28] K. Krishnamoorthy, M. Veerapandian, K. Yun, and S. -J. Kim, "The chemical and structural analysis of graphene oxide with different degrees of oxidation". *Carbon*, vol. 53, no. 1, pp. 38-49, 2013.
- [29] H. H. Khadhim, and K. A. Saleh, "Removing of copper ions from industrial waste water using graphene oxide/chitosan nanocomposite". *Iraqi Journal of Science*, vol. 63, no. 5, pp. 1894-1908, 2022.
- [30] R. Chuah, S. C. Gopinath, P. Anbu, M. N. Salimi, A. R. W. Yaakub, and T. LakshmiPriya, "Synthesis and Characterization of reduced graphene oxide using the aqueous extract of *Eclipta prostrata*". *3 Biotech*, vol. 10, no. 364, pp. 1-10, 2020.
- [31] E. Vatandost, A. Ghorbani-HasanSaraei, F. Chekin, S. N. Raeisi, and S. -A. Shahidi, "Green tea extract assisted green synthesis of reduced graphene oxide: Application for highly sensitive electrochemical detection of sunset yellow in food products". *Food Chemistry: X*, vol. 6, no. 100085, pp. 1-25, 2020.
- [32] S. Mahata, A. Sahu, P. Shukla, A. Rai, M. Singh, and V. K. Rai, "The novel and efficient reduction of graphene oxide prepared using *Ocimum sanctum* L. leaf extract as an alternative

- renewable bio-resource". *New Journal of Chemistry*, vol. 42, no. 24, pp. 19945-19952, 2018.
- [33] Y. -G. Yuan, and S. Gurunathan, "Combination of graphene oxide–silver nanoparticle nanocomposites and cisplatin enhances apoptosis and autophagy in human cervical cancer cells". *International Journal of Nanomedicine*, vol. 12, pp. 6537-6558, 2017.
- [34] H. A. Hessain, and J. J. Hassan, "Green synthesis of reduced graphene oxide using ascorbic acid". *Iraqi Journal of Science*, vol. 61, no. 6, pp. 1313-1319, 2020.
- [35] V. Loryuenyong, K. Totepvimarn, P. Eimburanaprat, W. Boonchompoo, and A. Buasri, "Preparation and characterization of reduced graphene oxide sheets via water-based exfoliation and reduction methods". *Advances in Materials Science and Engineering*, vol. 2013, no. 9, pp. 1-5, 2013.
- [36] J. Wang, E. C. Salihi, and L. Šiller, "Green reduction of graphene oxide using alanine". *Materials Science and Engineering: C*, vol. 72, no. 2017, pp. 1-6, 2017.
- [37] M. Khan, A. H. Al-Marri, M. Khan, N. Mohri, S. F. Adil, A. Al-Warthan, M. R. H. Siddiqui, H. Z. Alkathlan, R. Berger and W. Tremel, "Pulicaria glutinosa plant extract: a green and eco-friendly reducing agent for the preparation of highly reduced graphene oxide". *RSC Advances*, vol. 4, no. 46, pp. 24119-24125, 2014.
- [38] N. Zaaba, K. Foo, U. Hashim, S. Tan, W. -W. Liu, and C. Voon, "Synthesis of graphene oxide using modified hummers method: solvent influence". *Procedia Engineering*, vol. 184, no.1, pp. 469-477, 2017.
- [39] D. Chen, L. Li, and L. Guo, "An environment-friendly preparation of reduced graphene oxide nanosheets via amino acid". *Nanotechnology*, vol. 22, no.325601, pp. 1-7, 2011.
- [40] G. Lee, and B. S. Kim, "Biological reduction of graphene oxide using plant leaf extracts". *Biotechnology progress*, vol. 30, no.2, pp. 463-469, 2014.
- [41] M. Mahiuddin, and B. Ochiai, "Lemon juice assisted green synthesis of reduced graphene oxide and its application for adsorption of methylene blue". *Technologies*, vol. 9, no. 96, pp. 1-20, 2021.
- [42] O. Akhavan, M. Kalaei, Z. Alavi, S. M. A. Ghiasi and A. Esfandiari, "Increasing the antioxidant activity of green tea polyphenols in the presence of iron for the reduction of graphene oxide". *Carbon*, vol. 50, no. 8, pp. 3015-3025, 2012.
- [43] C. Li, Z. Zhuang, X. Jin and Z. Chen, "A facile and green preparation of reduced graphene oxide using Eucalyptus leaf extract". *Applied Surface Science*, vol. 422, no.1, pp. 469-474, 2017.
- [44] M. H. Raheema, "Coating of carbon nanotubes using chemical method of enhance the corrosion protecting of copper and aluminum metals in seawater medium". *Iraqi Journal of Science*, vol. 64, no.5, pp. 2117-2128, 2023.
- [45] A. K. Bidan, and Z. S. A. Al-Ali, "Biomedical evaluation of biosynthesized silver nanoparticles by Jasminum Sambac (L.) Aiton against breast cancer cell line, and both bacterial strains colonies". *International Journal of Nanoscience*, vol. 21, no. 6, pp. 1-15, 2022.
- [46] A. K. Bidan, and Z. S. A. Al-Ali, "Oleic and palmitic acids with derivatives essential oils synthesized of spherical gold nanoparticles and its anti-human breast carcinoma MCF-7 in vitro examination". *BioNanoScience*, pp. 1-14, 2023.
- [47] C. K. Chua, and M. Pumera, "Chemical reduction of graphene oxide: a synthetic chemistry viewpoint". *Chemical Society Reviews*, vol. 43, no. 1, pp. 291-312, 2014.
- [48] U. Waiwijit, W. Kandhavivorn, B. Oonkhanond, T. Lomas, D. Phokaratkul, A. Wisitsoraat, and A. Tuantranont, "Cytotoxicity assessment of MDA-MB-231 breast cancer cells on screen-printed graphene-carbon paste substrate". *Colloids and Surfaces B: Biointerfaces*, vol. 113, no.1, pp. 190-197, 2014.
- [49] A. B. Seabra, A. J. Paula, R. de Lima, O. L. Alves, and N. Durán, "Nanotoxicity of graphene and graphene oxide". *Chemical Research in Toxicology*, vol. 27, no. 2, pp. 159-168, 2014.
- [50] E. Vatandost, A. G. H. Saraei, F. Chekin, S. N. Raeisi, and S. A. Shahidi, "Antioxidant, antibacterial and anticancer performance of reduced graphene oxide prepared via green tea extract assisted biosynthesis". *ChemistrySelect*, vol. 5, no. 33, pp. 10401-10406, 2020.